Check for updates

Dialysis-derived urchin-like supramolecular assembly of tannic acid and paclitaxel with high porosity†

Jiyeon Kim, Chanuk Choi and Seonki Hong ⬤ *

Co-crystallization of active pharmaceutical ingredients (APIs) with pharmaceutically acceptable additives has emerged as an alternative to current drug delivery systems for hydrophobic drugs, due to their high drug loading efficiency. During this process, we herein report that tannic acid (TA) can be used as an amphiphilic stabilizer for the model drug, paclitaxel (PTX), that results in the shape and morphology variations of the synthesized microstructures, depending on the synthetic environment. We observed that rapid co-precipitation of PTX and TA *via* dialysis in water resulted in unprecedented urchin-like supramolecular microstructures with high porosity. On the other hand, slow co-precipitation for several hours under static conditions without dialysis exhibited bundles of straight TA-coated PTX fibers without any pores. This was plausibly due to the dynamic change of both the building block concentration and the solvent composition occurring during the transition of the kinetic product to the thermodynamic product. Interestingly, the synthesized urchin-like porous structure further rapidly transformed into a spherical shape through the interaction with serum proteins by remodeling of the non-covalent interactions, which contributed to the overall therapeutic efficacy tested *in vitro*. Our results provide knowledge on the self-assembly behavior of the hydrophobic drug and amphiphilic stabilizer under dynamic conditions, and contribute to the development of novel strategies in designing drug formulations.

Department of Emerging Materials Science, DGIST, Daegu, 42988, Republic of Korea.
E-mail: seonkihong@dgist.ac.kr
†Electronic supplementary information (ESI) available: Supporting figures. See DOI: 10.1039/d1nr06237a

Dr Seonki Hong received her Ph.D. degree in chemistry from KAIST in 2015 and worked as a postdoctoral fellow in the Center for Systems Biology at Massachusetts General Hospital from 2015 to 2017. Starting in June 2017, she joined the Department of Emerging Materials Science at DGIST as an assistant professor. Her research interests mainly focus on the development of nature-inspired catecholic and polyphenolic materials for bio-medical applications.

Seonki Hong

Introduction

Poor solubility is one of the major obstacles to achieving sufficient bioavailability of many clinical drugs. To solve this issue, various strategies have been suggested, including co-administration with organic solvents and surfactants, formulation with biopolymers, encapsulation in carriers such as liposomes, micelles, and nano-to-micron particles.[1] Although many of these strategies have succeeded in improving the water solubility/dispersibility and biostability, the combination with additives (1) increases the potential of severe side effects, and (2) inevitably reduces the drug loading efficiency, which overall limits the therapeutic efficacy. Co-crystallization of active pharmaceutical ingredients (APIs) with pharmaceutically acceptable additives has emerged as an alternative to these approaches due to their high drug content.[2] These can be synthesized either by top-down (ball-milling, high-pressure homogenization, and others) or bottom-up (antisolvent precipitation, spray drying, and others) routes.[2] In various synthetic routes, the size and shape of crystals, surface morphology, and surface hydrophilicity are factors that can determine the overall biodistribution and biostability.[3]

Tannic acid (TA) is a representative of tannins, a group of polyphenols that are ubiquitously found as secondary metab-

olites in plants. It has been therapeutically used due to its antioxidant, anticancer, and antiviral properties.[4,5] Recently, TA has also attracted considerable attention as a molecular building block in the construction of multifunctional nanoparticles, fibers, and coatings due to its multiple phenolic subunits that can participate in various molecular interactions, including metal coordination, π–π stacking, and hydrogen bonding.[6–8] Liu *et al.* showed that TA can self-assemble into various structures, such as cuboids, ovals, and spheres in binary solvents consisting of an organic solvent (methanol, isopropanol, pyridine, and tetrahydrofuran) and water.[9] Similarly, Allais *et al.* synthesized TA-based nanofibers by electrospinning in a water–ethanol cosolvent.[10] The fiber diameter was directly correlated with the mixing ratio of water and ethanol, and the synthesized nanofibers could be further crosslinked by either $NaIO_4$ or Fe(III) ions, enhancing the stability/durability. F. Caruso's group has developed various multifunctional nano-to-micro architectures by constructing metal–phenolic networks (MPNs) of various metal ions and polyphenolic compounds.[11,12] Given the advantage of the reversibility of the metal coordination bonds, these show pH-responsive properties.[13–15] By participating in various molecular interactions, TA can also be easily complexed with a variety of additives, which provide a useful tool kit for smart drug delivery systems. TA is known to solubilize various hydrophobic drugs such as curcumin, amphotericin B, DTX, rapamycin, and paclitaxel (PTX).[16] Chowdhury *et al.* reported that TA-complexed spherical nanoparticles of PTX show improved therapeutic efficacy over that of the free drug, since TA inhibits the P-gp efflux by partially inhibiting the ATPase.[17] Le *et al.* showed that nano-complexation with TA allows the oral administration of PTX with enhanced bioavailability.[18] Finally, Shin *et al.* reported a novel strategy of delivering cargos including AAV9, therapeutic peptide, and basic fibroblast growth factor (bFGF) into the heart by nano-complexation with TA, because TA shows unique affinity to the myocardium extracellular matrix.[19]

Herein, we report an unprecedented urchin-like microstructure of PTX with high porosity, synthesized by employing tannic acid (TA) as an amphiphilic stabilizer. During co-precipitation of PTX with TA, we found that dialysis resulted in dramatic shape changes compared to static incubation. Note that the shape of the drug crystal is one of the critical factors determining the bioavailability and therapeutic efficacy. Dialysis is a dynamic process that rapidly removes building blocks while they are participating in self-assembly. Therefore, it provides a completely different synthetic environment compared to conventional self-assemblies, in which the building block concentrations are often defined from the initial to the final stage. In addition, rapid solvent to anti-solvent conversion can also be incorporated during dialysis, which induces rapid precipitation synthesizing API crystals. Our mechanistic study indicates that this dynamic environment during dialysis plausibly affects the porosity of the supramolecular assembled PTX/TA complex as it transforms from the initial spherical shape (kinetic product) to the urchin-like fibrous structure

(thermodynamic product). The high porosity of the synthesized PTX/TA complex contributes to the rapid complexation with serum proteins, which is promising for prolonged intravascular retention and increased drug efficacy.

Results and discussion

Fig. 1A presents the synthetic scheme of urchin-like PTX/TA microstructures. PTX and TA were first dissolved and mixed in ethanol (a good solvent for both PTX and TA), and the mixture was co-precipitated by adding water (EtOH : water = 6 : 15) under vigorous sonication (for 5 min). Immediately after that, the solution was further dialyzed in water (a bad solvent for PTX) for 24 h. The microstructures of various shapes and densities were synthesized depending on the mixing ratio of TA and PTX after dialysis, imaged by conventional light microscopy (Fig. 1B). As the TA concentration (equivalent to PTX) increased, the overall yield decreased (Fig. S1†), as expected from the amphiphilic nature of TA, making PTX solubilize more in water, which enabled its easy removal during dialysis. Interestingly, conditions with lower TA (0.5–1 equiv. to PTX) resulted in straight fibrous shapes similar to the structures made from PTX without TA, and urchin-like structures were obtained by using more TA than PTX (2–8 equiv. to PTX) (Fig. 1B).

We next dropped the dialyzed solution on the Si wafer and dried it in air to investigate the microstructure by SEM imaging. Similar to the light microscopy images, urchin-like structures were observed when a high amount of TA was used (2–8 equiv. to PTX), and straight fibers intercrossing each other were detected when a low amount of TA was used (0.5–1 equiv. to PTX) (Fig. 2A, 1st row). This fiber intercrossing phenomenon was similar to the previously reported self-assembly of PTX in an ethanol–water cosolvent.[20] The urchin-like structure could also be understood along with this fiber intercrossing, but in this case, the growth of each strand was suppressed by the interaction with TA during dialysis. It was also reported that TA itself could be grown into anisotropic cuboid structures in a binary solvent consisting of ethanol and water,[9] but the intersection between fibers was not observed in the previous study. Interestingly, the structures synthesized under high TA conditions showed high porosity on each strand, but PTX-like fibers did not (Fig. 2A, 2nd row). The size of urchin-like microstructures was further quantified. The synthesized structures were heterogeneous under all conditions with different TA and PTX ratios, but could be grouped into two classes: one with urchin-like structures (class 1) and the other with structures made of straight fibers intercrossing at the middle (class 2), regardless of their porosity (Fig. 2B). The structures belonging to class 1 possess more strands and show an overall aspect ratio close to 1, while the structures in class 2 possess fewer strands and show an overall aspect ratio above 1 with high variation (Fig. S2†). An increase in the amount of TA resulted in a preference for the synthesis of structures belonging to class 1 as opposed to class 2; when more than 2 equiva-
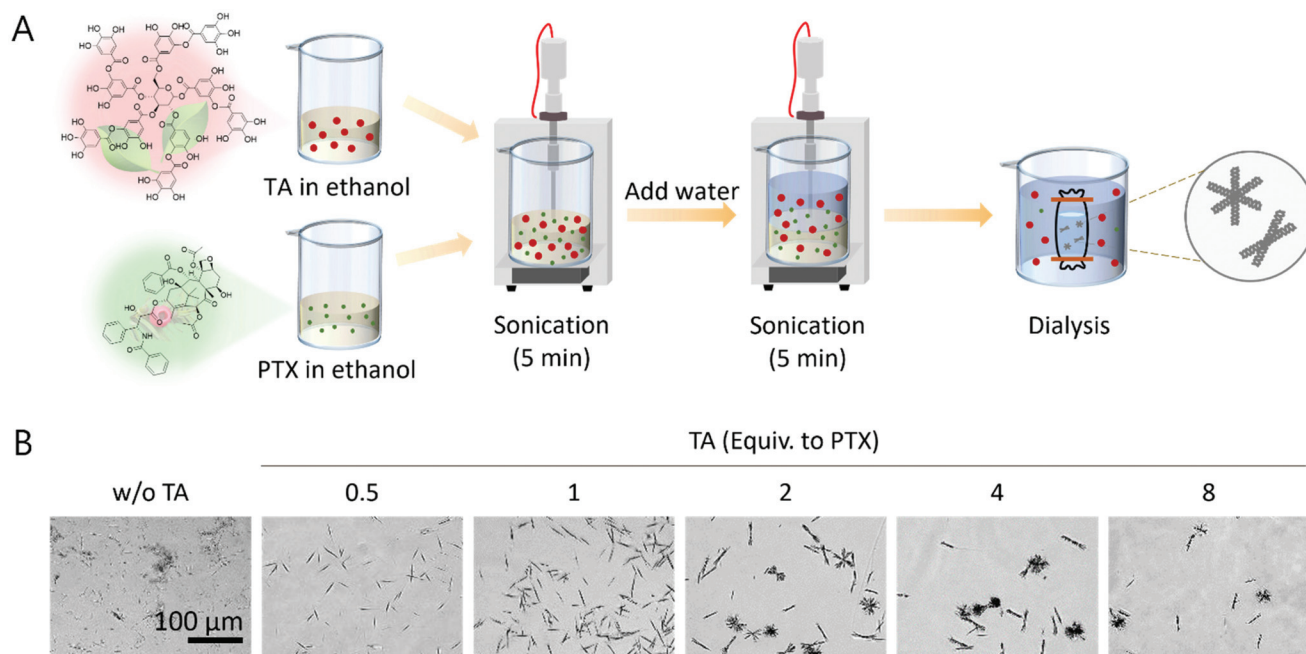
Fig. 1 Synthesis of the dialysis-driven PTX/TA co-precipitate. (A) Schematic illustrating the synthetic procedure of PTX/TA complexes through anti-solvent precipitation during the dialysis process. (B) Microscopic images showing the unprecedented urchin-like microstructures depending on the concentration of TA equivalent to PTX used during the synthesis.

lents of TA to PTX were used during synthesis, approximately 60% of the structures belonged to class 1 (Fig. 2C and Fig. S3†). In addition, as more TA was used during the synthesis, the lateral size of each structure decreased, and the width of individual strands in each structure increased (Fig. 2D). Finally, the loading of PTX under each condition was evaluated. As shown in Fig. 2E, more PTX was loaded in the complex when less TA was initially used. It is plausible that a high concentration of amphiphilic TA solubilizes the PTX more, resulting in easy removal during dialysis.

The porosity of the PTX/TA complexes synthesized at high TA (more than 2 equivalents to PTX) was unprecedented. We, therefore, further investigated how the porosity was generated. During the synthesis of these structures, as described in Fig. 1A, the mixture of TA and PTX in ethanol was immediately co-precipitated by the addition of water, followed by the immediate dialysis in water. On the other hand, we monitored the shape of the particles generated in the mixture of TA and PTX after adding water under static conditions without immediate dialysis, at this time. As shown in Fig. 3A, spherical particles were synthesized surrounding a fiber, imaged after air drying the solution after each period of incubation under static conditions up to 20 min. Further incubation over 20 min resulted in a sudden shape change; particles completely disappeared and bundles of straight intercrossing microfibers were observed instead. These fibers did not show any pores and further grew over 300 μm in length as the incubation time increased under static conditions (Fig. S4†). We then further investigated this phenomenon after dialyzing the particles and fibers synthesized under static conditions at each period of

incubation. As shown in Fig. 3B, the porosity generated after dialysis directly correlates with the initial structure of the PTX/TA complex formed under static conditions after each period of incubation without dialysis; initial conditions showing spherical particles synthesized under static conditions transformed into urchin-like structures with microporosity after dialysis, while straight fibers synthesized under static conditions did not change their structure even after dialysis. Once synthesized, the microstructures with high porosity were stable enough to be dried and redispersed (Fig. S5†). From this study, we can suggest a plausible mechanism for the synthesis of urchin-like structures with microporosity driven by dialysis at the moment when their thermodynamically stable assembly is not complete (Fig. 3C). Spherical particles are generated right after the co-precipitation of PTX and TA in the ethanol and water cosolvent, but these are not thermodynamically static. Therefore, they start to reassemble into straight fibrous structures during static incubation in the cosolvent. Once the fiber without porosity is formed after several minutes under static conditions, its shape does not further change even by dialysis, as this fibrous structure is a thermodynamic product. It is plausible that the fiber possesses a core–shell structure with a hydrophobic PTX core and an amphiphilic TA shell, based on the previous study regarding the self-assembly of PTX and the amphiphilic poly(ethylene glycol)-*block*-poly (lactide) polymer.[21,22] This was confirmed by X-ray diffraction (XRD) that the fibrous structures without porosity grown for 5 h under static conditions (denoted as T5) showed almost the same XRD pattern, probably from the PTX core, as PTX alone (Fig. S6,† pink). On the other hand, immediate dialysis
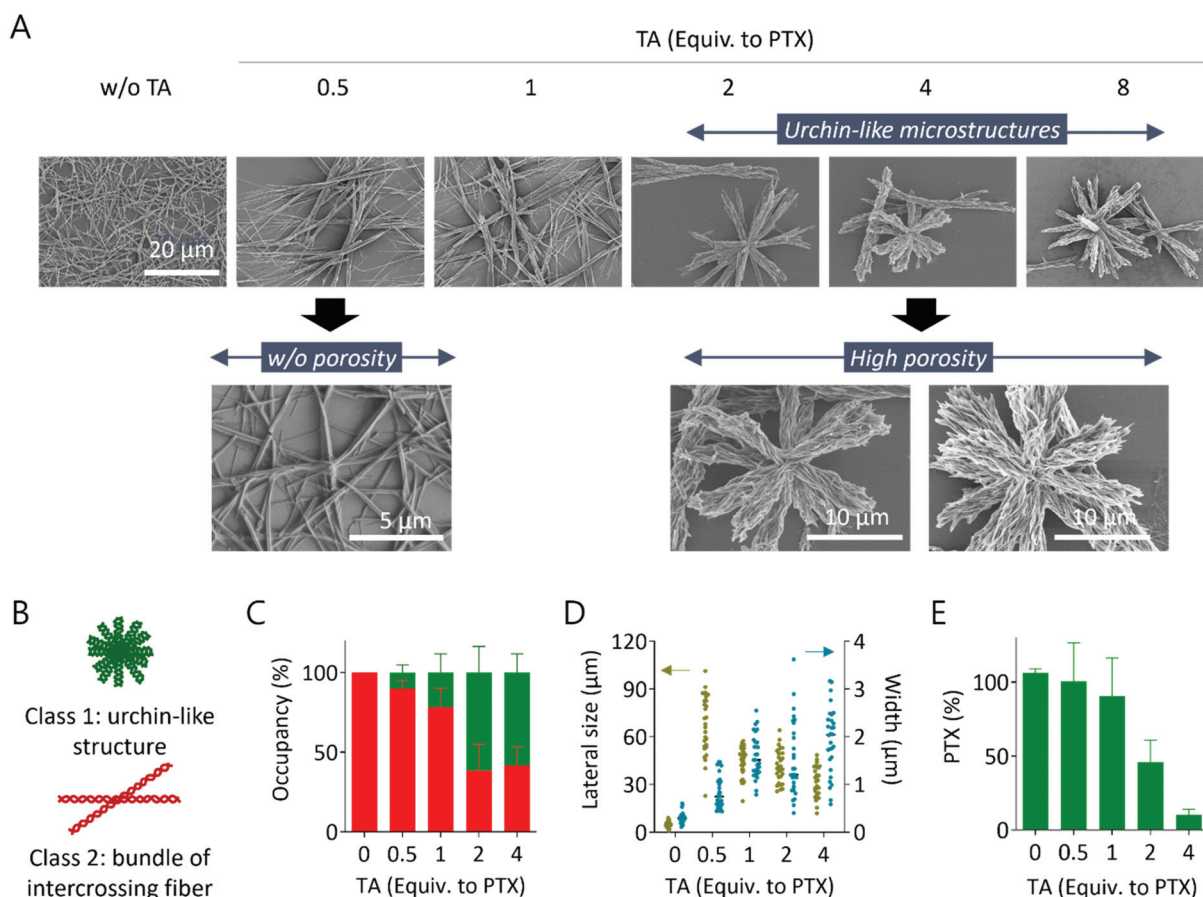
Fig. 2 Analysis of microstructures synthesized from various TA : PTX ratios. (A) SEM images of the synthesized PTX/TA complexes after dialysis, showing two distinct shapes shown in (B). (C) Occupancy of two distinct microstructures synthesized under each synthetic condition with different TA : PTX ratios. (D) Lateral size of microstructures and width of individual strands in microstructures synthesized under each synthetic condition with different TA : PTX ratios. (E) Loading efficiency of therapeutic PTX in each complex.

induces (1) a sudden reduction in the number of PTX and TA to be reassembled in the reaction medium, (2) a sudden increase in the water portion of the cosolvent, and (3) finally generates flow dynamics before the transition of the kinetic product to the thermodynamic product is complete, occasionally resulting in unprecedented porosity. However, it turned out that this environmental change during dialysis did not alter the core@shell structures. The XRD pattern of urchin-like structures with high porosity synthesized by immediate dialysis after mixing (denoted as T0) was almost the same as those of T5 and PTX alone (Fig. S6,† green). In addition, it was confirmed through NMR spectroscopy that although the porosity was completely different, their PTX content was similar; T0 contained 49% of PTX to the total mass, and T5 contained 54% of PTX to the total mass (Fig. S7†).

Interestingly, urchin-like microstructures with high porosity further rapidly reassembled in various solvents; they transformed into 1 μm-sized spherical particles when incorporated with serum proteins in 10% fetal bovine serum (FBS) and dissolved completely in DMSO (Fig. 4A). These results indicate that the major driving forces responsible for the synthesis of

the assembled structures are the various non-covalent interactions, including the hydrogen bond which is readily broken by DMSO intercalation. We expect that this reassembly with serum proteins will contribute to both the PTX releasing profile and the tumor accumulation *in vivo*. To validate this, the *in vitro* anticancer activity was evaluated on an MCF-7 breast cancer cell line (Fig. 4B). The PTX/TA microstructures were well dispersed in the cell media regardless of their microporosity, due to the amphiphilic nature of TA. Free PTX, however, was first dissolved in DMSO and then diluted in the cell media due to its low solubility in aqueous media (the final concentration of DMSO in the cell media was 0.3% v/v). It was confirmed that the microporosity of the PTX/TA complex highly contributed to the structural remodeling with proteins; as shown in Fig. 4B, the highly porous T0 complex showed comparable anticancer efficacy with free PTX, but the T5 complex without any micropores showed less anticancer activity due to its lower interaction with serum proteins. TA itself also possessed intrinsic anticancer activity (Fig. S8†), but it was negligible because the TA concentration in the tested PTX/TA complex was sufficiently low (approximately 1.25 μM).
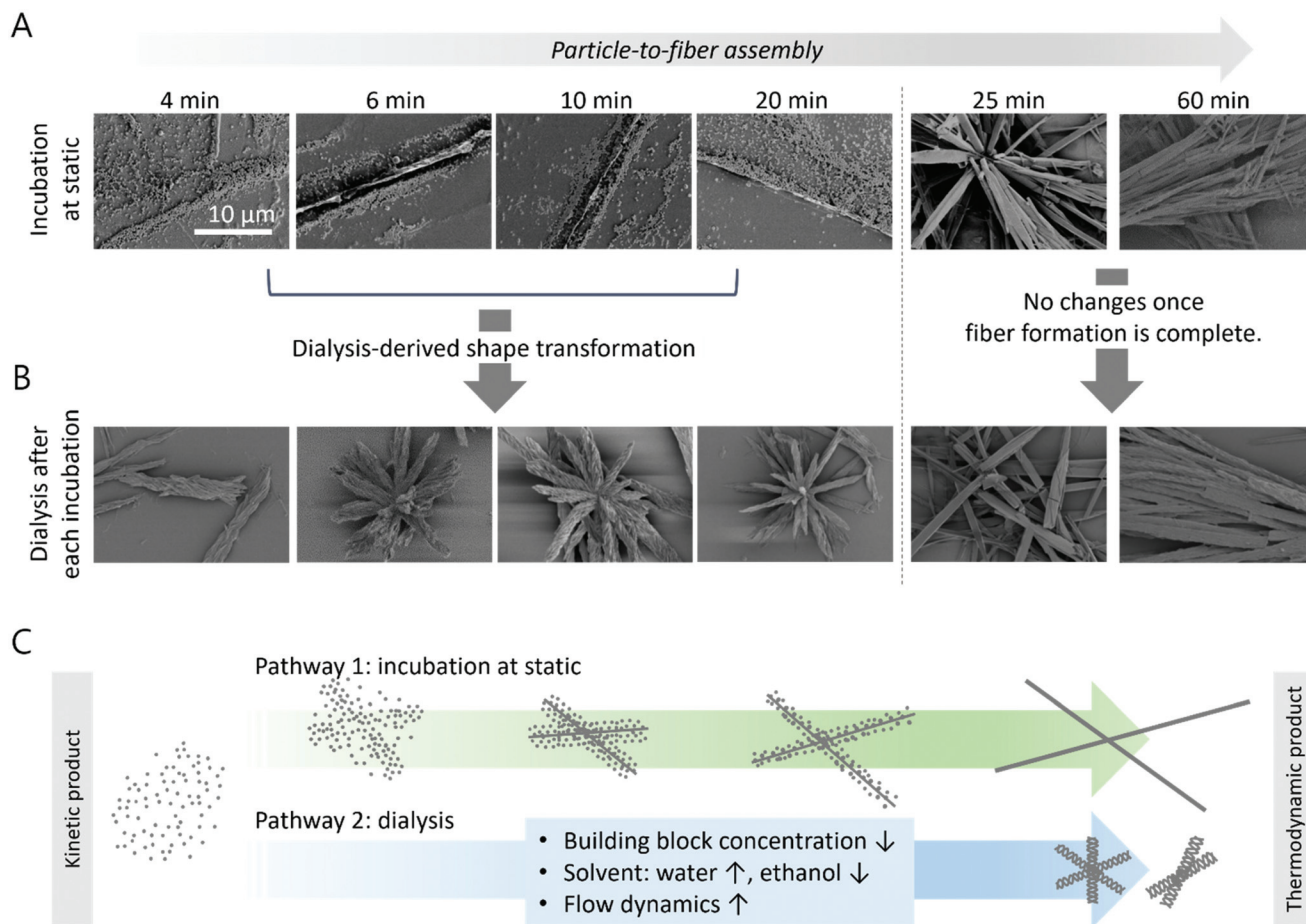
Fig. 3 Dialysis effect on the self-assembly of the PTX/TA complex during antisolvent precipitation. (A) Monitoring of the shape transformation from particles to fibers under static conditions without dialysis (2 equivalents of TA to PTX were used). (B) Results of dialysis-induced shape changes at each time point post-incubation. (C) Schematic illustration describing the effect of dialysis on the self-assembly of the PTX/TA complex.

Experimental

Materials and reagents

Paclitaxel (PTX) was purchased from LC laboratories®. Tannic acid (TA), dimethyl sulfoxide (DMSO), DMSO-d_6, and thiazolyl blue tetrazolium bromide (MTT) were purchased from Sigma-Aldrich. Ethanol (99.9%) was purchased from Duksan. Deionized water (DW) (Milli-Q®) with a conductivity of 18.2 MΩ was used in the preparation of all aqueous solutions. Fetal bovine serum (FBS), 1× phosphate buffered saline (1× PBS), and penicillin–streptomycin were purchased from Corning®. Roswell Park Memorial Institute (RPMI)-1640 was purchased from Hyclone®. A Spectrum™ Spectra/Por™ 4 RC dialysis membrane tubing (12–14 kDa MWCO) was used for dialysis.

Synthesis of PTX/TA microstructures

PTX (3 mL; 1 mg mL^{-1} in ethanol) was mixed with TA (3 mL; 0, 0.5, 1, 2, 4, 8 and 1 mg mL^{-1} in ethanol) under vigorous sonication for 5 min (1 s on, 1 s off, 30% power amplitude). Subsequently, DW (15 mL) was added to the mixture under vigorous sonication for another 5 min (1 s on, 1 s off, 40% power

amplitude). The mixture was then dialyzed against DW for 24 h (MWCO = 12–14 kDa) (denoted as the T0 condition). For the synthesis of PTX/TA structures without porosity, the whole mixture was dialyzed after 5 h post-incubation under static conditions (denoted as the T5 condition). An ultra-sonicator (KFS-1200N from Korea Process Technology Co., Ltd) was used for all mixing processes.

Characterization

For SEM imaging, the dialyzed solutions containing PTX/TA complexes were directly dropped onto the Si wafer and air dried. Scanning electron microscopy (SEM) was performed using an ultra-high-resolution field emission SEM (S-4800, Hitachi) after platinum sputtering the sample for 30 s at 15 mA. To compare the chemical compositions of T0 and T5, ^{1}H-NMR analysis was performed using a Bruker AVANCE III 400 spectrometer after lyophilization of the dialyzed PTX/TA complexes and then redispersion in DMSO-d_6 (5 mg mL^{-1}). To measure the PTX content in the PTX/TA complex, the dialyzed solution containing the PTX/TA complex was directly mixed with methanol (1 : 3 v/v) and analyzed by high-performance
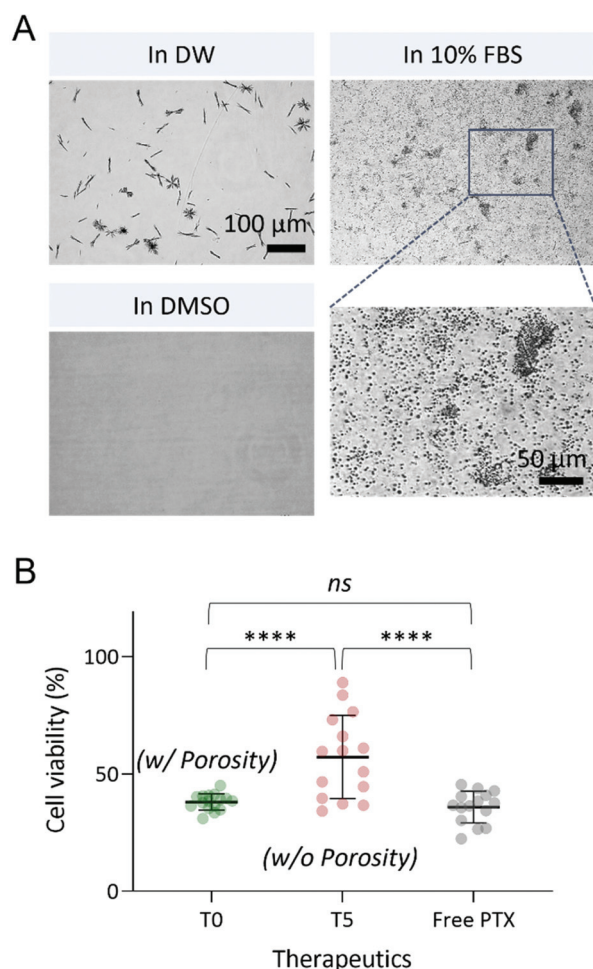
Fig. 4 *In vitro* therapeutic efficacy. (A) Shape remodeling of urchin-like structures in 10% FBS and DMSO. (B) *In vitro* anticancer activity on the MCF-7 breast cancer cell line. All samples possessed the same PTX concentration (1.25 μM). T0 denotes the microstructure synthesized by immediate dialysis resulting in high porosity, and T5 denotes the structure dialyzed after 5 h post-incubation under static conditions possessing no porosity. Data are expressed as the mean $\pm$ SD, ns >0.05 and p**** < 0.0001 (one-way ANOVA with a *post hoc* Dunnett's test, n = 15–16 per group).

liquid chromatography spectrometry (HPLC-DAD) (6420, Agilent Technologies) using a C18 column. A 6 : 4 mixture of acetonitrile and distilled water was used as an eluent, and the flow rate was 0.2 mL min^{-1}.

Cell culture

The breast cancer cell line (MCF-7) was purchased from the Korean Cell Line Bank. MCF-7 cells were cultivated in an RPMI-1640 medium containing 10% fetal bovine serum (FBS) and 1% penicillin. The cells were maintained in 5% CO_2 at 37 °C with humidity and passaged at 80% confluency.

In vitro anticancer activity

To assess the cytotoxicity of the PTX/TA complex, an MTT assay was performed in the MCF-7 cell line following the man-

ufacturer's procedure. Briefly, 1×10^4 cells were seeded in a 96-well plate and incubated for 24 h. Next, the medium was replaced with 100 μL of fresh medium containing PTX/TA microstructures, the PTX content of which is equivalent to 1.25 μM, and then incubated for 72 h. As a positive control, 1.25 μM with free-PTX in medium containing 0.3% DMSO was used. Then, 10 μL of MTT reagent was directly added to the medium and incubated for 4 h. Finally, the medium was completely discarded, and the remaining formazan was dissolved in 100 μL of DMSO, and its absorbance at 520 nm was measured using a microplate reader.

Conclusions

In this study, we investigated the dialysis effect on the complexation of a model hydrophobic drug, PTX, and a nature-derived amphiphilic stabilizer, TA. Under static conditions without dialysis, the co-precipitate of PTX and TA in a binary solvent of ethanol and water transformed from a spherical kinetic product at the initial stage to a fibrous thermodynamic product within several minutes. During this process, dialysis could be applied to induce dynamic changes in (1) the building block concentration, (2) the solvent–antisolvent composition, and (3) the flow stream, which resulted in unprecedented urchin-like microstructures with high porosity. The optimized structure was approximately 30 μm in lateral size and contained over 45% of PTX. This size was larger than conventional drug formulations, but owing to non-covalent interactions between PTX and TA, it rapidly re-shaped into 1 μm-sized spherical particles with the incorporation of serum proteins when dissolved in 10% FBS. Highly porous urchin-like structures showed high anticancer activity due to this reshaping, but non-porous fibrous structures did not. Our results provide an insight into the design of novel formulations of hydrophobic drugs *via* the antisolvent precipitation method by indicating how dynamic environments such as dialysis affect the self-assembly of hydrophobic drugs and additives.

Conflicts of interest

There are no conflicts to declare.

Acknowledgements

References

1 S. Kalepu and V. Nekkanti, Insoluble drug delivery strategies: review of recent advances and business prospects, *Acta Pharm. Sin. B*, 2015, **5**, 442–453.

2 T. Domenech and P. S. Doyle, High loading capacity nanoencapsulation and release of hydrophobic drug nanocrystals from microgel particles, *Chem. Mater.*, 2020, **32**, 498–509.

3 Y. Lu, Y. Li and W. Wu, Injected nanocrystals for targeted drug delivery, *Acta Pharm. Sin. B*, 2016, **6**, 106–113.

4 B. Kaczmarek, Tannic Acid with Antiviral and Antibacterial Activity as A Promising Component of Biomaterials—A Minireview, *Materials*, 2020, **13**, 3224.

5 P. Buzzini, P. Arapitsas, M. Goretti, E. Branda, B. Turchetti, P. Pinelli, F. Ieri and A. Romani, Antimicrobial and Antiviral Activity of Hydrolysable Tannins, *Mini-Rev. Med. Chem.*, 2008, **8**, 1179–1187.

6 D. Wu, J. Zhou, M. N. Creyer, W. Yim, Z. Chen, P. B. Messersmith and J. V. Jokerst, Phenolic-enabled nanotechnology: versatile particle engineering for biomedicine, *Chem. Soc. Rev.*, 2021, **50**, 4432–4483.

7 H. Moon, J. Kim and S. Hong, Plant-derived polyphenol-based nanomaterials for drug delivery and theranostics, in *Bioinspired and Biomimetic Materials for Drug Delivery*, ed. Md. Nurunnabi, Elsevier, 2021, pp. 39–54, ISBN: 978-0-12-821352-0.

8 R. Lu, X. Zhang, X. Cheng, Y. Zhang, X. Zan and L. Zhang, Medical Applications Based on Supramolecular Self-Assembled Materials from Tannic Acid, *Front. Chem.*, 2020, **8**, 583484.

9 Z. Liu, H. Fan, W. Li, G. Bai, X. Li, N. Zhao, J. Xu, F. Zhou, X. Guo, B. Dai, E. Benassi and X. Jia, Competitive self-assembly driven as a route to control the morphology of poly(tannic acid) assemblies, *Nanoscale*, 2019, **11**, 4751.

10 M. Allais, D. Mailley, P. Hébraud, D. Ihiawakrim, V. Ball, F. Meyer, A. Hébraud and G. Schlatter, Polymer-free electrospinning of tannic acid and cross-linking in water for hybrid supramolecular nanofibers, *Nanoscale*, 2018, **10**, 9164.

11 H. Ejima, J. J. Richardson, K. Liang, J. P. Best, M. P. Van Koeverden, G. K. Such, J. Cui and F. Caruso, One-step assembly of coordination complexes for versatile film and particle engineering, *Science*, 2013, **341**, 154–157.

12 H. Ejima, J. J. Richardson and F. Caruso, Metal-phenolic networks as a versatile platform to engineer nanomaterials and biointerfaces, *Nano Today*, 2017, **12**, 136–148.

13 J. Chen, S. Pan, J. Zhou, R. Seidel, S. Beyer, Z. Lin, J. J. Richardson and F. Caruso, Metal–Phenolic Networks as Tunable Buffering Systems, *Chem. Mater.*, 2021, **33**, 2557–2566.

14 J. Chen, S. Pan, J. Zhou, Q.-Z. Zhong, Y. Qu, J. J. Richardson and F. Caruso, Programmable Permeability of Metal–Phenolic Network Microcapsules, *Chem. Mater.*, 2020, **32**, 6975–6982.

15 Q. A. Besford, Y. Ju, T.-Y. Wang, G. Yun, P. V. Cherepanov, C. E. Hagemeyer, F. Cavalieri and F. Caruso, Self-Assembled Metal-Phenolic Networks on Emulsions as Low-Fouling and pH-Responsive Particles, *Small*, 2018, **14**, 1802342.

16 J. K. Jackson and K. Letchford, The Effective Solubilization of Hydrophobic Drugs Using Epigallocatechin Gallate or Tannic Acid-Based Formulations, *J. Pharm. Sci.*, 2016, **105**, 3143–3152.

17 P. Chowdhury, P. K. B. Nagesh, E. Hatami, S. Wagh, N. Dan, M. K. Tripathi, S. Khan, B. B. Hafeez, B. Meibohm, S. C. Chauhan, M. Jaggi and M. M. Yallapu, Tannic acid-inspired paclitaxel nanoparticles for enhanced anticancer effects in breast cancer cells, *J. Colloid Interface Sci.*, 2019, **535**, 133–148.

18 Z. Le, Y. Chen, H. Han, H. Tian, P. Zhao, C. Yang, Z. He, L. Liu, K. W. Leong, H.-Q. Mao, Z. Liu and Y. Chen, Hydrogen-Bonded Tannic Acid-Based Anticancer Nanoparticle for Enhancement of Oral Chemotherapy, *ACS Appl. Mater. Interfaces*, 2018, **10**, 42186–42197.

19 M. Shin, H.-A. Lee, M. Lee, Y. Shin, J.-J. Song, S.-W. Kang, D.-H. Nam, E. J. Jeon, M. Cho, M. Do, S. Park, M. S. Lee, J.-H. Jang, S.-W. Cho, K.-S. Kim and H. Lee, Targeting protein and peptide therapeutics to the heart via tannic acid modification, *Nat. Biomed. Eng.*, 2018, **2**, 304–317.

20 A. Dev, A. Sood, S. R. Choudhury and S. Karmakar, Paclitaxel nanocrystalline assemblies as a potential trans-catheter arterial chemoembolization (TACE) candidate for unresectable hepatocellular carcinoma, *Mater. Sci. Eng., C*, 2020, **107**, 110315.

21 X. D. Guo, J. P. K. Tan, S. H. Kim, L. J. Zhang, Y. Zhang, J. L. Hedrick, Y. Y. Yang and Y. Qian, Computational studies on self-assembled paclitaxel structures: templates for hierarchical block copolymer assemblies and sustained drug release, *Biomaterials*, 2009, **30**, 6556–6563.

22 J. P. K. Tan, S. H. Kim, F. Nederberg, E. A. Appel, R. M. Waymouth, Y. Zhang, J. L. Hedrick and Y. Y. Yang, Hierarchical supermolecular structures for sustained drug release, *Small*, 2009, **5**, 1504–1507.